

# Neutron halo in deformed nuclei from a relativistic Hartree-Bogoliubov model in a Woods-Saxon basis

S G Zhou<sup>1,2</sup>, J Meng<sup>3,1,2</sup>, P Ring<sup>4,3</sup> and E G Zhao<sup>1,2,3</sup>

<sup>1</sup> Institute of Theoretical Physics, Chinese Academy of Sciences, Beijing 100190, China

<sup>2</sup> Center of Theoretical Nuclear Physics, National Laboratory of Heavy Ion Accelerator, Lanzhou 730000, China

<sup>3</sup> School of Physics, Peking University, Beijing 100871, China

<sup>4</sup> Physikdepartment, Technische Universität München, 85748 Garching, Germany

E-mail: sgzhou@itp.ac.cn

**Abstract.** Halo phenomenon in deformed nuclei is studied by using a fully self-consistent deformed relativistic Hartree-Bogoliubov model in a spherical Woods-Saxon basis with the proper asymptotic behavior at large distance from the nuclear center. Taking a deformed neutron-rich and weakly bound nucleus  $^{44}\text{Mg}$  as an example and by examining contributions of the halo, deformation effects, and large spatial extensions, we show a decoupling of the halo orbitals from the deformation of the core.

## 1. Introduction

Since it was first observed in the weakly bound system  $^{11}\text{Li}$  [1], halo phenomenon has been one of the most interesting topics in nuclear physics. Much effort has been focused on the investigation of the structure and dynamics of nuclear halo [2]. Since most open shell nuclei are deformed, the interplay between deformation and weak binding raises interesting questions, such as whether or not there exist halos in deformed nuclei and, if yes, what are their new features.

Calculations in a deformed single-particle model with the spin-orbit coupling neglected have shown that valence particles in specific orbitals with low projection of the angular momentum on the symmetry axis can give rise to halo structures in the limit of weak binding and the deformation of the halo may be different from that of the core [3]. Halos in deformed nuclei were investigated in several mean field calculations [4, 5, 6]. However, there are some doubt about the occurrence of halos in deformed nuclei. For example, it has been concluded that in the neutron orbitals of an axially deformed Woods-Saxon potential the lowest- $\ell$  component becomes dominant at large distances from the origin and therefore all  $\Omega^\pi = 1/2^+$  levels do not contribute to deformation for binding energies close to zero [7]. In addition, a three-body model study [8] suggests that it is unlikely to find halos in deformed drip line nuclei because the correlations between the nucleons and those due to static or dynamic deformations of the core inhibit the formation of halos.

In order to give an adequate description of halos in deformed nuclei, a model should be used which includes in a self-consistent way the continuum, deformation effects, large spatial distributions, and couplings among all these features. Spherical nuclei with halos have been described in the past successfully by the solution of either the non-relativistic Hartree-Fock-Bogoliubov (HFB) [9, 10, 11] or the relativistic Hartree Bogoliubov (RHB) equations [12, 13, 14]

in coordinate ( $r$ ) space. However, for deformed nuclei the solution of HFB or RHB equations in  $r$  space is a numerically very demanding task. In the past considerable effort has been made to develop mean field models either in  $r$  space or in a basis with an improved asymptotic behavior at large distances [6, 15, 16, 17, 18, 19, 20, 21]. In Ref. [18] the Woods-Saxon basis was proposed as a reconciler between the harmonic oscillator basis and coordinate space. The Woods-Saxon wave functions have more realistic asymptotic behavior at large  $r$  than the harmonic oscillator wave functions do. One can use a box boundary condition to discretize the continuum. It has been shown that the results in a Woods-Saxon basis is almost equivalent to those obtained in  $r$  space [18, 22, 23]. A deformed relativistic Hartree model (DRH) [24] and a deformed relativistic Hartree-Bogoliubov model (DRHB) [25] in a Woods-Saxon basis have also been developed.

In a recent work [26], the halo phenomenon in deformed nuclei is studied by using the DRHB model in a Woods-Saxon basis. In this contribution, we shall present some of the results on neutron halo in deformed nuclei. The formalism of the DRHB model in a Woods-Saxon basis will be given in section 2. In section 3, the results and discussions will be presented. Finally a summary is given.

## 2. The deformed relativistic Hartree-Bogoliubov model in a Woods-Saxon basis

The RHB equation for the nucleons reads [27]

$$\sum_{\sigma'p'} \int d^3\mathbf{r}' \begin{pmatrix} h_D(\mathbf{r}\sigma p, \mathbf{r}\sigma'p') - \lambda & \Delta(\mathbf{r}\sigma p, \mathbf{r}'\sigma'p') \\ -\Delta^*(\mathbf{r}\sigma p, \mathbf{r}'\sigma'p') & -h_D(\mathbf{r}\sigma p, \mathbf{r}\sigma'p') + \lambda \end{pmatrix} \begin{pmatrix} U_k(\mathbf{r}'\sigma'p') \\ V_k(\mathbf{r}'\sigma'p') \end{pmatrix} = E_k \begin{pmatrix} U_k(\mathbf{r}\sigma p) \\ V_k(\mathbf{r}\sigma p) \end{pmatrix}, \quad (1)$$

where  $p = 1, 2$  is used to represent the particle-antiparticle degree of freedom,  $E_k$  is the quasiparticle energy,  $\lambda$  is the Fermi energy, and  $h_D$  is the Dirac Hamiltonian [28, 29, 30, 31, 32],

$$h_D = \boldsymbol{\alpha} \cdot \mathbf{p} + V(\mathbf{r}) + \beta(M + S(\mathbf{r})). \quad (2)$$

The pairing potential reads

$$\Delta(\mathbf{r}_1\sigma_1p_1, \mathbf{r}_2\sigma_2p_2) = \sum_{\sigma'_1p'_1}^{\sigma'_2p'_2} V_{p_1p_2p'_1p'_2}(\mathbf{r}_1, \mathbf{r}_2; \sigma_1\sigma_2\sigma'_1\sigma'_2) \kappa(\mathbf{r}_1\sigma'_1p'_1, \mathbf{r}_2\sigma'_2p'_2). \quad (3)$$

For axially deformed nuclei with spacial reflection symmetry, we expand the potentials and the densities in terms of the Legendre polynomials [33],

$$f(\mathbf{r}) = \sum_{\lambda} f_{\lambda}(r) P_{\lambda}(\cos \theta), \quad \lambda = 0, 2, 4, \dots \quad (4)$$

The quasiparticle wave function is expanded in terms of wave functions of the Dirac Woods-Saxon basis  $\{\epsilon_{i\kappa m}, \varphi_{i\kappa m}(\mathbf{r}\sigma p)\}$  as,

$$U_k(\mathbf{r}\sigma p) = \sum_{i\kappa} \begin{pmatrix} u_{k,(i\kappa)}^{(m)} \varphi_{i\kappa m}(\mathbf{r}\sigma p) \\ u_{k,(\tilde{i}\kappa)}^{(\tilde{m})} \tilde{\varphi}_{i\kappa m}(\mathbf{r}\sigma p) \end{pmatrix}, \quad V_k(\mathbf{r}\sigma p) = \sum_{i\kappa} \begin{pmatrix} v_{k,(i\kappa)}^{(m)} \varphi_{i\kappa m}(\mathbf{r}\sigma p) \\ v_{k,(\tilde{i}\kappa)}^{(\tilde{m})} \tilde{\varphi}_{i\kappa m}(\mathbf{r}\sigma p) \end{pmatrix}. \quad (5)$$

The basis wave function reads

$$\varphi_{i\kappa m}(\mathbf{r}\sigma) = \frac{1}{r} \begin{pmatrix} iG_{i\kappa}(r) Y_{jm}^l(\Omega\sigma) \\ -F_{i\kappa}(r) Y_{jm}^l(\Omega\sigma) \end{pmatrix}, \quad j = l \pm \frac{1}{2}, \quad (6)$$

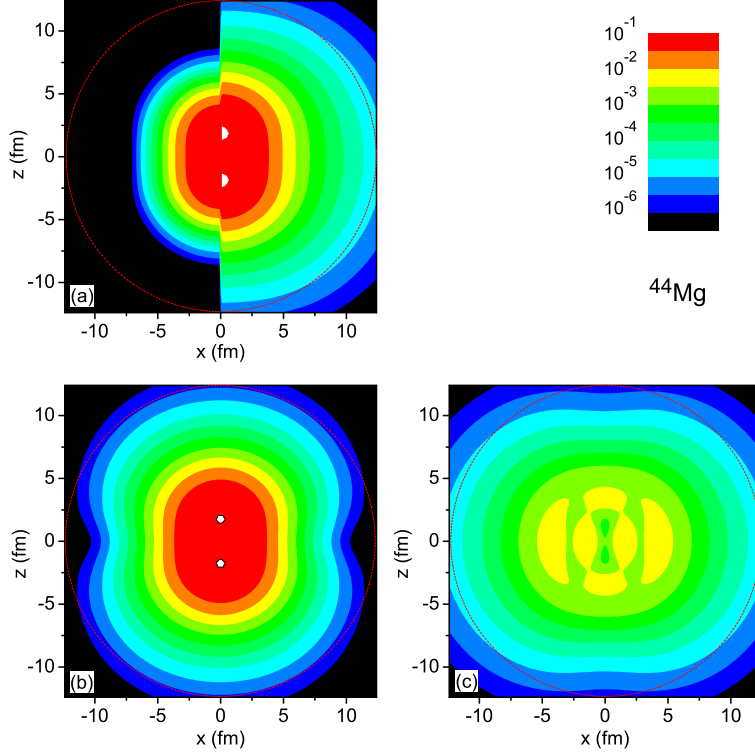


**Figure 1.** (Color online) Density distributions of  $^{44}\text{Mg}$  with the  $z$ -axis as symmetry axis: (a) the proton density (for  $x < 0$ ) and the neutron density (for  $x > 0$ ), (b) the density of the neutron core, and (c) the density of the neutron halo. In each plot, a dotted circle is drawn for guiding the eye. This figure is originally published in Ref. [26].

with  $G_{i\kappa}(r)/r$  and  $F_{i\kappa}(r)/r$  the radial wave functions for the upper and lower components and  $Y_{jm}^l$  the spinor spherical harmonics where  $\kappa = (-1)^{j+l+1/2}(j+1/2)$  and  $\tilde{l} = l + (-1)^{j+l-1/2}$ .  $\tilde{\varphi}_{i\kappa m}(\mathbf{r}\sigma p)$  is the time reversal state of  $\varphi_{i\kappa m}(\mathbf{r}\sigma p)$ . The states both in the Fermi sea and in the Dirac sea should be included in the basis for the completeness [18, 34]. For each  $m$ -block, solving the RHB equation (1) is equivalent to the diagonalization of the matrix,

$$\begin{pmatrix} \mathcal{A} & \mathcal{B} \\ \mathcal{C} & \mathcal{D} \end{pmatrix} \begin{pmatrix} \mathcal{U} \\ \mathcal{V} \end{pmatrix} = E \begin{pmatrix} \mathcal{U} \\ \mathcal{V} \end{pmatrix}, \quad (7)$$

where

$$\mathcal{U} = \left( u_{k,(i\kappa)}^{(m)} \right), \quad \mathcal{V} = \left( v_{k,(\tilde{i}\kappa)}^{(m)} \right), \quad (8)$$

$$\mathcal{A} = \left( A_{(i\kappa)(i'\kappa')}^{(m)} \right), \quad \mathcal{D} = \left( -A_{(\tilde{i}\kappa)(\tilde{i}'\kappa')}^{(m)} \right), \quad (9)$$

$$\mathcal{B} = \left( \Delta_{(i\kappa)(\tilde{i}'\kappa')}^{(m)} \right), \quad \mathcal{C} = \left( -\Delta_{(\tilde{i}\kappa)(i'\kappa')}^{(m)} = \Delta_{(i'\kappa')(\tilde{i}\kappa)}^{(m)} \right). \quad (10)$$

For the pp channel, we use a zero range density dependent force,

$$V_{p_1 p_2 p'_1 p'_2}(\mathbf{r}_1, \mathbf{r}_2; \sigma_1 \sigma_2 \sigma'_1 \sigma'_2) = \frac{1}{4} V_0 \delta(\mathbf{r}_1 - \mathbf{r}_2) \left( 1 - \frac{\rho(\mathbf{r}_1)}{\rho_{\text{sat}}} \right) [1 - 4 \vec{\sigma}_{11'} \cdot \vec{\sigma}_{22'}] [\mathbf{I}_{11'}^p \cdot \mathbf{I}_{22'}^p]. \quad (11)$$

### 3. Results and discussions

The calculations are based on the density functional NL3 [35]. For the pp interaction (11), the following parameters are used:  $\rho_{\text{sat}} = 0.152 \text{ fm}^{-3}$  and  $V_0 = 380 \text{ MeV}\cdot\text{fm}^3$ , and a cut-off energy  $E_{\text{cut}}^{\text{q.p.}} = 60 \text{ MeV}$  is applied in the quasi-particle space. These parameters were fixed by reproducing the proton pairing energy of the spherical nucleus  $^{20}\text{Mg}$  obtained from a spherical

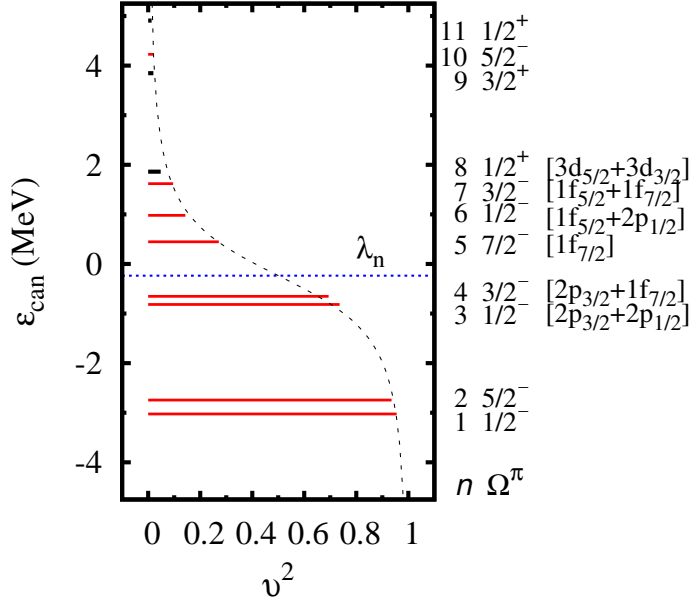


**Figure 2.** (Color online) Single neutron levels with the quantum numbers  $\Omega^\pi$  around the chemical potential (dotted line) in the canonical basis for  $^{44}\text{Mg}$  as a function of the occupation probability  $v^2$ . The order  $n$ ,  $\Omega^\pi$ , and the main Woods-Saxon components for orbitals close to the threshold are also given. The dashed line corresponds to the BCS-formula with an average pairing gap. This figure is originally published in Ref. [26].

relativistic Hartree-Bogoliubov calculation with the Gogny force D1S. A spherical box of the size  $R_{\text{max}} = 20$  fm and the mesh size  $\Delta r = 0.1$  fm are used for generating the spherical Dirac Woods-Saxon basis [18] which consists of states with  $j < \frac{21}{2}\hbar$ . An energy cutoff  $E_{\text{cut}}^+ = 100$  MeV is applied to truncate the positive energy states in the Woods-Saxon basis and the number of negative energy states in the Dirac sea is taken to be the same as that of positive energy states in each  $(\ell, j)$ -block.

In the DRHB calculations for magnesium isotopes, the last nucleus within the neutron drip-line is  $^{46}\text{Mg}$  which is almost spherical. The neighboring even-even nucleus  $^{44}\text{Mg}$  is well deformed with quadrupole deformation  $\beta_2 = 0.32$ . This nucleus is weakly bound with a small two-neutron separation energy  $S_{2n} = 0.44$  MeV. Since we are interested in the neutron halo in deformed unstable nuclei,  $^{44}\text{Mg}$  is taken as an example for a detailed investigation. The density distributions of all protons and all neutrons in this nucleus are shown in Figure 1(a). Due to the large neutron excess, the neutron density not only extends much farther in space but also shows a halo structure. The neutron density is decomposed into the contribution of the core in Figure 1(b) and that of the halo in Figure 1(c). Details of this decomposition are given later. It is seen that the core of  $^{44}\text{Mg}$  is prolately deformed, but the halo has a slightly oblate deformation, which indicates the decoupling between the deformations of core and halo.

To study the formation mechanism of a nuclear halo, one needs to investigate the weakly bound orbitals and/or those embedded in the continuum. For an intuitive understanding of the single particle structure we keep in mind that HB-wave functions can be represented by BCS-wave functions in the canonical basis and show in Figure 2 the corresponding single particle spectrum for the neutrons. As discussed in Ref. [36] the single particle energies in the canonical basis  $\varepsilon_k = \langle k | h_D | k \rangle$  shown in Figure 2 are expectation values of the Dirac Hamiltonian (2) for the eigenstates  $|k\rangle$  of the single particle density matrix  $\hat{\rho}$  with the eigenvalues  $v_k^2$ . The discrete part of the spectrum of  $\hat{\rho}$  with  $v_k^2 > 0$  contributes to the HB-wave function and only this part is plotted in Figure 2. This part of the spectrum  $\varepsilon_k$  is discrete even for the levels in the continuum. Of course, this is only possible because the wave functions  $|k\rangle$  are not eigenfunctions of the Hamiltonian. As long as the Fermi energy  $\lambda_n$  is negative, the corresponding density  $\rho(\mathbf{r})$  is localized and the particles occupying the levels in the continuum are bound [10].

The orbitals in Figure 2 are labeled by the conserved quantum numbers  $\Omega$  and  $\pi$ . The character  $n$  numbers the different orbitals appearing from the bottom to the top in this figure

according to their energies. The neutron Fermi energy lies within the  $pf$  shell and most of the single particle levels have negative parities. Since the chemical potential  $\lambda_n = -230$  keV is relatively small, the orbitals above the threshold have noticeable occupation probabilities due to pairing correlations. For example, the occupation probabilities of the 5th ( $\Omega^\pi = 7/2^-$ ) and the 6th ( $\Omega^\pi = 1/2^-$ ) orbitals are 27.2% and 14.3%, respectively.

As we see in Figure 2 there is a considerable gap between the two levels with the numbers  $n = 2$  and  $n = 3$ . The levels with  $\varepsilon_{\text{can}} < -2.5$  MeV contribute to the “core”, and the other remaining weakly bound and continuum orbitals with  $\varepsilon_{\text{can}} > -1$  MeV naturally form the “halo”. Therefore we decompose the neutron density into two parts, one part coming from the orbitals with canonical single particle energies  $\varepsilon_{\text{can}} < -2.5$  MeV (called “core”) and the other from the remaining weakly bound and continuum orbitals (called “halo”). A further decomposition of the neutron density shows that the two weakly bound orbitals, i.e., the 3rd ( $\Omega^\pi = 1/2^-$ ) and the 4th ( $\Omega^\pi = 3/2^-$ ), contribute mostly to the halo. If we decompose the deformed wave functions of the two weakly bound orbitals, i.e. the 3rd ( $\Omega^\pi = 1/2^-$ ) and the 4th ( $\Omega^\pi = 3/2^-$ ), in the spherical Woods-Saxon basis it turns out that in both cases the major part comes from  $p$  waves as indicated on the right hand side of Figure 2. The low centrifugal barrier for the  $p$  wave gives rise to the formation of the halo. Having a small  $p$  wave component, the 6th orbital ( $\Omega^\pi = 1/2^-$ ) contributes less to the halo though it is in the continuum and the occupation probability is rather large. The contribution of the 8th orbital ( $\Omega^\pi = 1/2^+$ ) to the tail of the density is even smaller because its main components are of  $d$  waves. The large centrifugal barrier of  $f$  states hinders strongly the spatial extension of the wave functions of the other two continuum orbitals, i.e., the 5th ( $\Omega^\pi = 7/2^-$ ) and the 7th ( $\Omega^\pi = 3/2^-$ ).

The slightly oblate shape of the halo originates from the intrinsic structure of the weakly bound and continuum orbitals. As is mentioned above and shown in Figure 2, the main Woods-Saxon components of the two weakly bound orbitals, the 3rd ( $\Omega^\pi = 1/2^-$ ) and the 4th ( $\Omega^\pi = 3/2^-$ ), are  $p$  states. We know that the angular distribution of  $|Y_{10}(\theta, \phi)|^2 \propto \cos^2 \theta$  with a projection of the orbital angular momentum on the symmetry axis  $\Lambda = 0$  is prolate and that of  $|Y_{1\pm 1}(\theta, \phi)|^2 \propto \sin^2 \theta$  with  $\Lambda = 1$  is oblate. It turns out that in the 3rd ( $\Omega^\pi = 1/2^-$ ) orbital, both  $\Lambda = 0$  and  $\Lambda = 1$  components contribute and the latter dominates. Therefore this orbital has a slightly oblate shape. For the 4th ( $\Omega^\pi = 3/2^-$ ) state, there is only the  $\Lambda = 1$  component from the  $p_{3/2}$  wave, an oblate shape is also expected.

#### 4. Summary

Neutron halo in deformed nuclei is investigated within a deformed relativistic Hartree Bogoliubov model in a Woods-Saxon basis. In a very neutron-rich deformed nucleus  $^{44}\text{Mg}$  a pronounced deformed neutron halo is found. It is formed by several orbitals close to the threshold. These orbitals have large components of low  $\ell$ -values and feel therefore only a small centrifugal barrier. Although  $^{44}\text{Mg}$  and its core are prolately deformed, the deformation of the halo is slightly oblate. This implies a decoupling between the shapes of the core and the halo. The mechanism is investigated by studying the details of the neutron densities for core and halo, the single particle levels in the canonical basis, and the decomposition of the halo orbitals. We also studied the weakly-bound nuclei in Ne isotopes and discussed the conditions for the occurrence of a halo and the shape decoupling [26]. It is shown that the existence and the deformation of a possible neutron halo depends essentially on the quantum numbers of the main components of the single particle orbits in the vicinity of the Fermi surface.

#### Acknowledgments

This work has been supported in part by Natural Science Foundation of China (10775004, 10705014, 10875157, and 10979066), Major State Basic Research Development Program of China (2007CB815000), Knowledge Innovation Project of Chinese Academy of Sciences (KJ CX3-SYW-

N02 and KJCX2-YW-N32), by the Bundesministerium für Bildung und Forschung (BMBF), Germany, under Project 06 MT 246, and by the DFG cluster of excellence “Origin and Structure of the Universe” ([www.universe-cluster.de](http://www.universe-cluster.de)). The computation was supported by Supercomputing Center, CNIC of CAS.

## References

- [1] Tanihata I, Hamagaki H, Hashimoto O, Shida Y, Yoshikawa N, Sugimoto K, Yamakawa O, Kobayashi T and Takahashi N 1985 *Phys. Rev. Lett.* **55** 2676–2679
- [2] Jensen A S, Riisager K, Fedorov D V and Garrido E 2004 *Rev. Mod. Phys.* **76** 215–261
- [3] Misu T, Nazarewicz W and Åberg S 1997 *Nucl. Phys. A* **614** 44–70
- [4] Li X and Heenen P H 1996 *Phys. Rev. C* **54** 1617–1621
- [5] Pei J, Xu F and Stevenson P 2006 *Nucl. Phys. A* **765** 29–38
- [6] Nakada H 2008 *Nucl. Phys. A* **808** 47–59
- [7] Hamamoto I 2004 *Phys. Rev. C* **69** 041306R–4
- [8] Nunes F 2005 *Nucl. Phys. A* **757** 349–359
- [9] Bulgac A 1980 Hartree-Fock-Bogoliubov approximation for finite systems IPNE FT-194-1980, Bucharest (arXiv: nucl-th/9907088)
- [10] Dobaczewski J, Flocard H and Treiner J 1984 *Nucl. Phys. A* **422** 103–139
- [11] Dobaczewski J, Nazarewicz W, Werner T R, Berger J F, Chinn C R and Dechargé J 1996 *Phys. Rev. C* **53** 2809–2840
- [12] Meng J and Ring P 1996 *Phys. Rev. Lett.* **77** 3963–3966
- [13] Pöschl W, Vretenar D, Lalazissis G A and Ring P 1997 *Phys. Rev. Lett.* **79** 3841–3844
- [14] Meng J 1998 *Nucl. Phys. A* **635** 3–42
- [15] Terasaki J, Heenen P H, Flocard H and Bonche P 1996 *Nucl. Phys. A* **600** 371–386
- [16] Stoitsov M V, Dobaczewski J, Ring P and Pittel S 2000 *Phys. Rev. C* **61** 034311–14
- [17] Teran E, Oberacker V E and Umar A S 2003 *Phys. Rev. C* **67** 064314–13
- [18] Zhou S G, Meng J and Ring P 2003 *Phys. Rev. C* **68** 034323–12
- [19] Tajima N 2004 *Phys. Rev. C* **69** 034305–22
- [20] Stoitsov M, Michel N and Matsuyanagi K 2008 *Phys. Rev. C* **77** 054301–12
- [21] Pei J C, Stoitsov M V, Fann G I, Nazarewicz W, Schunck N and Xu F R 2008 *Phys. Rev. C* **78** 064306–12
- [22] Schunck N and Egido J L 2008 *Phys. Rev. C* **77** 011301R–5
- [23] Schunck N and Egido J L 2008 *Phys. Rev. C* **78** 064305–14
- [24] Zhou S G, Meng J and Ring P 2006 *AIP Conf. Proc.* vol 865 ed Ma Y G and Ozawa A (AIP) pp 90–95
- [25] Zhou S G, Meng J and Ring P 2008 *Physics of Unstable Nuclei* ed Khoa D T, Egelhof P, Gales S, Van Giai N and Motobayashi T (World Scientific) pp 402–408 (arXiv: 0803.1376v1 [nucl-th])
- [26] Zhou S G, Meng J, Ring P and Zhao E G 2010 *Phys. Rev. C* **82** 011301R–5
- [27] Kucharek H and Ring P 1991 *Z. Phys. A* **339** 23–35
- [28] Serot B D and Walecka J D 1986 *Adv. Nucl. Phys.* **16** 1–327
- [29] Reinhard P G 1989 *Rep. Prog. Phys.* **52** 439–514
- [30] Ring P 1996 *Prog. Part. Nucl. Phys.* **37** 193–263
- [31] Vretenar D, Afanasjev A, Lalazissis G and Ring P 2005 *Phys. Rep.* **409** 101–259
- [32] Meng J, Toki H, Zhou S G, Zhang S Q, Long W H and Geng L S 2006 *Prog. Part. Nucl. Phys.* **57** 470–563
- [33] Price C E and Walker G E 1987 *Phys. Rev. C* **36** 354–364
- [34] Zhou S G, Meng J and Ring P 2003 *Phys. Rev. Lett.* **91** 262501–4
- [35] Lalazissis G A, König J and Ring P 1997 *Phys. Rev. C* **55** 540–543
- [36] Ring P and Schuck P 1980 *The Nuclear Many-Body Problem* (Springer)